6200
P_27

Geometrical Modelling of Textile Reinforcements

Christopher M. Pastore*   Alexander B. Birger   Eugene Clyburn

February 24, 1995

SUMMARY

The mechanical properties of textile composites are dictated by the arrangement of yarns contained within the material. Thus to develop a comprehensive understanding of the performance of these materials, it is necessary to develop a geometrical model of the fabric structure. This task is quite complex, as the fabric is made from highly flexible yarn systems which experience a certain degree of compressability. Furthermore there are tremdous forces acting on the fabric during densification typically resulting in yarn displacement and misorientation.

The objective of this work is to develop a methodology for characterizing the geometry of yarns within a fabric structure including experimental techniques for evaluating these models. Furthermore, some applications of these geometric results to mechanical property predictions models are demonstrated.

Although more costly than its predecessors, the present analysis is based on the detailed architecture developed by one of the authors and his colleagues [1, 2] and accounts for many of the geometric complexities that other analyses ignore.

INTRODUCTION

While laminated composite materials have gained wide acceptance in aerospace and other industries, they do have disadvantages. Among these is a significant lack of damage tolerance. Because design allowables necessarily account for the performance of a damaged component, aircraft components made of laminated composites must be designed for maximum stresses or strains that are much lower than the undamaged strength of the materials. Textile composites offer significantly improved damage tolerance compared with traditional laminated materials though they do have decreased in-plane properties. However, since the residual strength of the damaged textile composite is typically higher than that of a corresponding laminate, the design allowables for the parts may actually be higher.

---

*North Carolina State University, College of Textiles

Traditional approaches to the study of textile based composite materials incorporate a type of volume averaging from the onset. They tend to be based on strength of materials and classical lamination theory, or a homogenized finite element approach [3, 4]. These models have been shown to work well for predicting gross elastic properties for many textile based materials, and, in some cases, provide reasonable estimates of material strength for simple textiles. However, even the finite element models consider the inhomogeneous materials either as voxels or as spars/beams in a matrix. The result is lack of ability to determine details of the internal response of these materials under load. Other failure models tend to be empirical [4], and because of the expense of developing a material database suitable for design, are often not flexible enough for practical use. A macro finite element approach [5] shows some details of load distribution within the composite, but even this analysis neglects many of the geometric details that affect the performance of the material.

As with any structural material, it is necessary to have a good understanding of the mechanical response and failure mechanisms. For textile reinforced composites, this ability has not yet been fully developed. In this paper, a method for analyzing the stress-strain state of a loaded textile composite material is presented. The proposed technique for the analysis of textile composites is based on a finite element discretization of detailed textile architectures.

Unlike previous attempts to determine the response of textile composites, this approach greatly reduces the geometric simplifications required for modeling. The finite element models are taken directly from Textile Geometry Models (TGM) and allow internal details of the response of representative structures to be examined. This paper focuses on the development of the models from the TGM phase through the development of the finite element model of a sample textile composite.

GEOMETRIC MODELLING

Although more costly in terms of computational resources, the present analysis, based on the representative volume element (RVE) of a textile composite, allows prediction of the load, mode, and location of failure initiation within the RVE. Through these models, not only is gross characterization possible, but internal details of displacement, strain, stress, and failure parameters can be studied. Specifically, this discussion focuses on the analysis of a plain weave textile composite. Linear elastic in-plane axial loading is considered.

It is clear that the mechanical response of a reinforced material is dependent upon the

type of reinforcement, constituent material properties, and the physical location and orientation of the reinforcing members. In the case of a textile reinforced composite, quantification of the geometrical properties of the reinforcement is rather complex. Thus, the first step in a detailed modeling approach is the development of methodologies for predicting and reporting the positions and orientation of the yarns contained within the RVE.

Theory and Discussion of TGM

Considering a yarn to contain typically 12,000 or more filaments, it is computationally efficient to consider the yarn as a continuum. The physical and mechanical properties of this yarn can be determined and predicted on the basis of the thousands of filaments, but the RVE analysis will be based on yarns as fundamental elements.

Thus the textile reinforcement can be considered as a collection of prismatic elements which bend, twist and undulate throughout the RVE. Ideally the yarn can also vary its cross-sectional shape (although not area) depending on transverse pressure, etc.

The analytical solution of this problem meets serious difficulties because of the large number of mechanisms involved in the deformation of a fabric, such as crimp exchange; thread shear; extension, bending, twisting and flattening of yarns; friction between yarns and others. Another obstacle is a large number of required parameters. For example, following [6], eleven parameters are needed in order to describe the geometry of a plain weave fabric and four to define the orthogonal components of stress and strain. Thus, the complete analysis of the fabric when considering all the parameters and mechanisms is an extremely complicated task. In order to predict mechanical behavior, varying degrees of simplification have been introduced. For example, in [6], among several other assumptions, the yarns are assumed to be circular.

In the present research, the geometrical and mechanical modeling is carried out on the structural level of the unit cell. The unit cell can be built from the segments of multiple yarns, where the number of yarn segments, their relative location, and the applied forces being entirely determined by fabric design.

The yarns forming a unit cell are considered to be elastic bodies interacting with one another and subject to external loads. The center line of every yarn is represented as a Bezier curve interpolating a set of discrete support points. In this study, a continuous Bezier with degree $n - 1$ (over n support points per yarn) was used. The location of the support points fully determines the current mechanical state of the unit cell. The yarns are assumed to have elliptical cross sectional shapes.

Lagrange's principle of minimum work is used to determine the mechanical equilibrium of the system. The following expression is used to represent the Lagrangian:

$$L = \sum_{i=1}^{N}(W_t^i + W_b^i + W_\theta^i) + W_{penalty} - A_{extern} \tag{1}$$

where

$$W_t^i = \int C_t^i \varepsilon_i^2 dl_i \tag{2}$$
$$W_b^i = \int C_b^i \kappa_i^2 dl_i$$
$$W_\theta^i = \int C_\theta^i \theta_i^2 dl_i$$

C_t^i, C_b^i, and C_θ^i correspond to tension, bending and twist coefficients of ith yarn, ε_i is the longitudinal strain, κ_i is the local curvature, and θ_i is the linear twist of the ith yarn. N represents the number of yarns forming the unit cell, l_i is the arc-length coordinate along the center line of ith yarn, W_p represents a penalty for volumetric intersection of yarns, and A_e is the work of applied external loads.

The Lagrangian (1) does not account for the dissipation of energy in the system. Of course, in the general case friction can be one of the major factors influencing the mechanics of the unit cell. It is important to note that there are no principal difficulties in introducing the corresponding friction term into the model.

The center lines of yarns are represented in the model by Bezier curves [7] interpolating sets of support points. In addition, a number of intermediate points placed on the center lines of yarns are selected. At any of these intermediate points tangent, normal and bi- normal vectors are built [8]. Ellipses located in the planes perpendicular to the center lines and containing intermediate points as their centers represent the surfaces of yarns.

In-plane orientation of axes of the ellipses and all three coordinates of support points are subject to variations in order to minimize L. After every variation and rebuilding of surfaces, all of the yarns are checked for mutual volumetric intersections. For this purpose, the surfaces each pair of yarns are rendered. For every encountered local intersection event extra penalty is added to L, the value of the penalty depending upon the dimensions of intersection volume. By choosing the corresponding penalty function it is possible to account indirectly for the energy of changing of the shape of the yarn cross section of two interacting yarns. For modeling of rigid yarns the penalty term should be equal to some sufficiently large value which will exclude any volumetric intersection of the yarns. The scanning of surfaces is the most complicated and numerically expensive portion of the algorithm. Only by assuming that all the yarns have circular cross-sections is it possible to escape computer scanning of surfaces and to apply some simpler method: scanning of center lines of every couple of yarns forming unit cell. But this assumption cannot be applied in many cases.

The work of external forces is defined as:

$$W_e = \sum_{i=1}^{N} (u_\alpha^i F_\alpha^i + u_\omega^i F_\omega^i) \tag{3}$$

where u_α^i and u_ω^i are displacement vectors of the beginning and the end point of the ith yarn, and F_α and F_ω are the external forces applied to these points.

There is one serious problem which appears when determining mechanical equilibrium of the unit cell. In general, the geometry model leads to mathematical task of finding the minimum of a multi-extremum function. Practically, any numerical algorithm for solving this task can converge to a local extremum which can result in the incorrect prediction of elastic properties of the fabric. In order to increase the probability of finding the state of the system corresponding to the global minimum of L, a number of techniques are known, but none of them can guarantee the convergence to the global minimum. For the problem under consideration the following method proved to be effective: the positions of several support points of different yarns are varied simultaneously during

a single step. In particular, two contacting yarns can be displaced together without penetrating one into another (this situation is one of the origins for local minima of L, and any variation of position of any single support point can be unable to reduce the Lagrangian).

GEOMETRY FROM FABRICATED MATERIALS

Having developed the previously described model for predicting the geometric structure of an arbitrary fabric, it is necessary to consider the quality of the results. This is accomplished by comparing the theoretical predictions with experimental results for a plain weave fabric.

Comparison of Experimental and Theoretical Results

One method of evaluating the effectiveness of this model is to consider the changes that occur to the fabric as a function of applied external load. This also allows the flexibility to incorporate forces associated with molding to the model. For this purpose, a set of data determined at NCSU[1] have been obtained by applying uni-axial tension to a specimen made of woven cloth. The properties of the specimen are described in Table 1.

A number of tensile tests have been performed on warp and weft yarns. The results are shown in Table 2

The parameters of the fabric (dimensions of yarns, distance between the yarns) and the results of testing, characterizing elastic properties of warp and weft yarns (C_t), have been taken as input data for the numerical phase of the geometrical analysis.

In order to simulate the experiment, a model representing four segments of yarns has been used. The geometry of the unit cell indicating the direction of forces applied to the ends of warp yarns in the warp direction are shown in Figure 1.

Initial geometry and applied loads

The minimization of Lagrangian (1) was performed for several different load values. When the applied load F is small (*i.e.* the work on the individual yarns is of the same order of magnitude as

---

[1]The experiments were performed by S. V. Pullela and Dr. B. S. Gupta of the College of Textiles, North Carolina State University.

the energy of tension for all yarns) the elongation of specimen in the warp direction occurs mostly due to the crimp interchange between warp and weft yarns, the length of warp yarns being almost unchanged. It corresponds to the initial nonlinear segment of stress-strain curve. When the applied loads are high, the warp yarns are almost straight, and the weft yarns are crimped. The elongation of the specimen occurs due to elongation of warp yarns, and the modulus is stiffer and close to linear.

As an example, the unit cell of the plain weave was solved for the case of nominal warp yarn loading (in this case, 25 grams applied to each warp yarn). The results are illustrated in Figure 1. As can be seen, the unit cell is symmetric, as expected.

When a greater load is applied (in this case 1,000 grams per warp yarn), there is tremendous crimp exchange, and much of the strain is due to reorientation of the yarns within the unit cell. The loaded unit cell is illustrated in Figure 2, and the dramatic differences in warp and weft yarn paths can be seen clearly.

During the minimization of L the out-of-plane (z) coordinates of the end points of both weft yarns and both warp yarns were kept unchanged. This allowed simulation of real boundary conditions of the experiment. The Poisson's effect in the specimen, neglected in this formulation of boundary conditions, is believed to be small because of the small distance between the jaws of the testing machine (2.0 cm). In addition, only those variations which do not violate the anti-symmetry of the unit cell with respect to its center were applied to the coordinates of support points.

Both experimental and analytical load-strain curves are shown in Figure 3 The values of applied external forces have been normalized by a number of warp yarns in the specimen. Good agreement between experimental and analytical curves which is seen in Figure 3 demonstrates the validity of the developed geometrical model.

Table 1: Parameters of Plain Weave Fabric Under Consideration

Picks per cm	17.7
Ends per cm	22.0
Crimp in the weft yarn	20%
Crimp in the warp yarn	3%
Denier (Weft)	567
Denier (Warp)	578

Table 2: Tensile properties of warp and weft yarns

Yarn	Number Tests	Average peak Load, (gf)	Average peak Strain (%)
Warp yarn	14	1021	29.64
Weft yarn	10	563.9	23.66
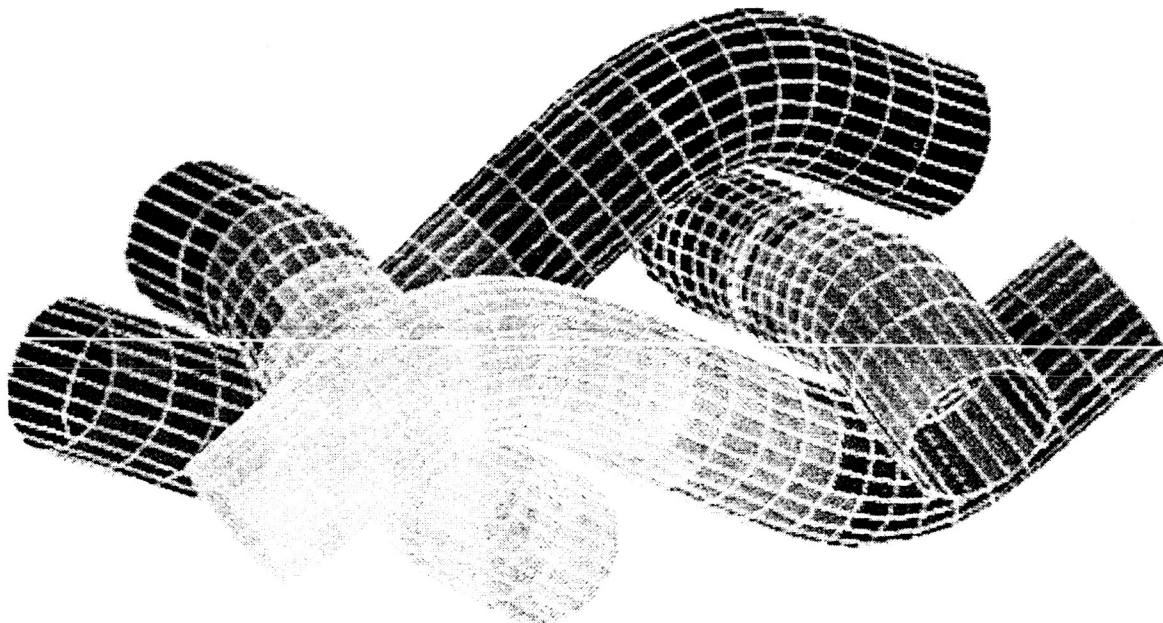
Figure 1: Graphical Rendering of Plain Weave Fabric With Nominal External Load (25 g) at Equilibrium
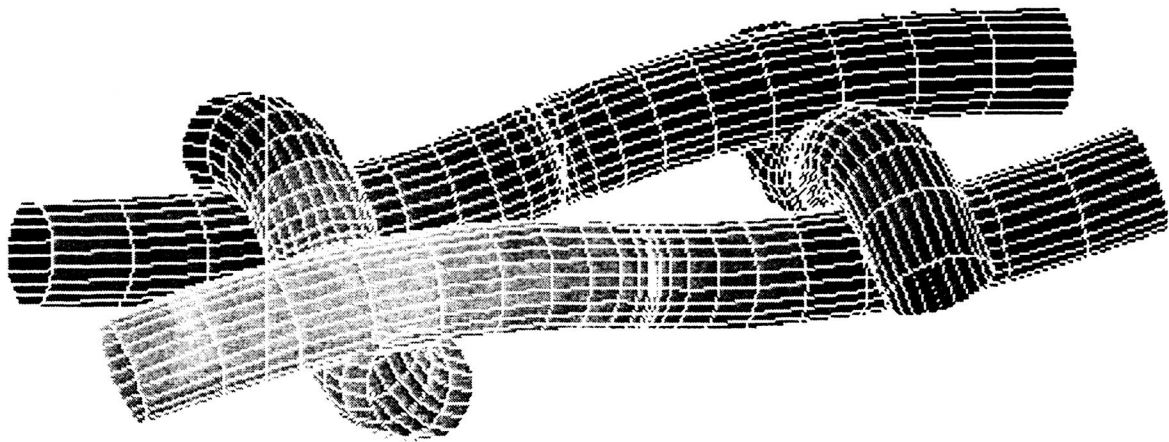
Figure 2: Graphical Rendering of Plain Weave Fabric With 1,000 Gram External Load at Equilibrium
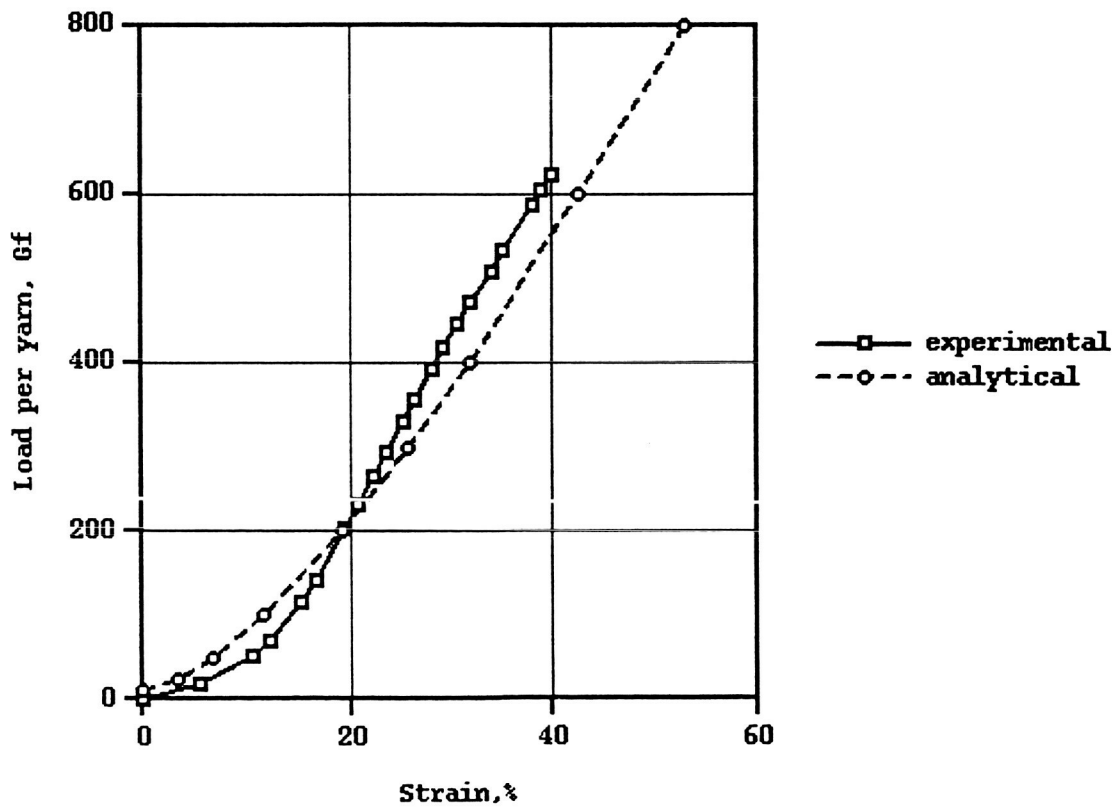

Figure 3: Comparison of Experimental and Predicted Axial Stress-Strain Response of Plain Weave Fabric

Although is can be shown that the model gives a good estimate of the geometrical properties of "dry" fabrics, even when exposed to external loading, for composite applications this fabric will be consolidated or densified with some matrix material. It is during this densification process that various misallignments can occur. Depending on the care taken when processing the material, the resultant composite may have good match with the geometrical predictions, or may have experienced significant skewing during formation.

Additionally, it is not uncommon to find fabrics with defects. A model of an ideal RVE necessarily does not include defects in the modeling. For the purposes of this paper ideal fabrics have been modeled, that is, the fabric structure contains no defects and there is no distortion or skewing of the fabric during densification. Furthermore it is assumed that there is no interlayer nesting in the stacked composite. Only a single layer composite is considered in the subsequent geometrical analysis.

NUMERICAL GEOMETRIC RESULTS

The analysis was performed for the four specific braids that are currently being tested as part of the overall NASA activity. These braids are characterized according to Table 3:

The yarns forming the analized fragment were assumed to have elliptical cross-sections with the ratio:

$$r_{major}/r_{minor} = 3$$

and with the cross-sectional area proportional to number of fibers in the yarn.

These data are represented graphically for LSS in Figures 4 and 5. Braid LLS is illustrated in Figures 6 and 7. Figures 8 and 9 show the geometry predictions for SLL. Braid LLL is not shown, as it is geometrically equivalent to SLL. The master sub-cell of each braid is shown in two different spatial orientations for visualization purposes.

Table 3: Braided Fabric Identification Scheme

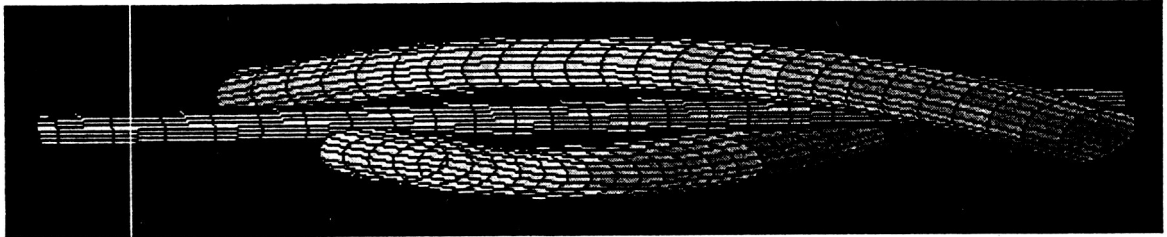| ID	Long. Size	θ size	θ	% Long.
LSS	6K	15K	45	12.0
LLS	36K	15K	45	46.0
SLL	30K	6K	70	46.0
LLL	75K	15K	70	46

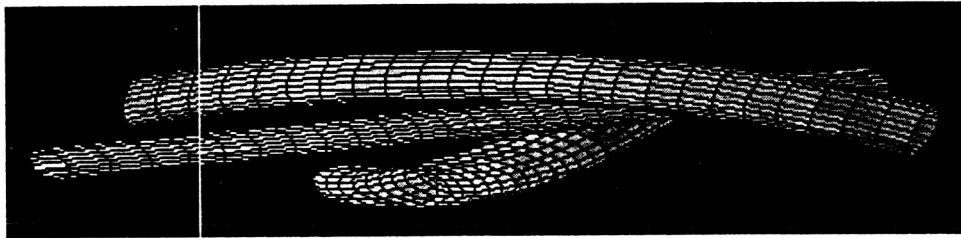Figure 4: Geometry of Triaxial Braid Model. *LSS*, Front View.

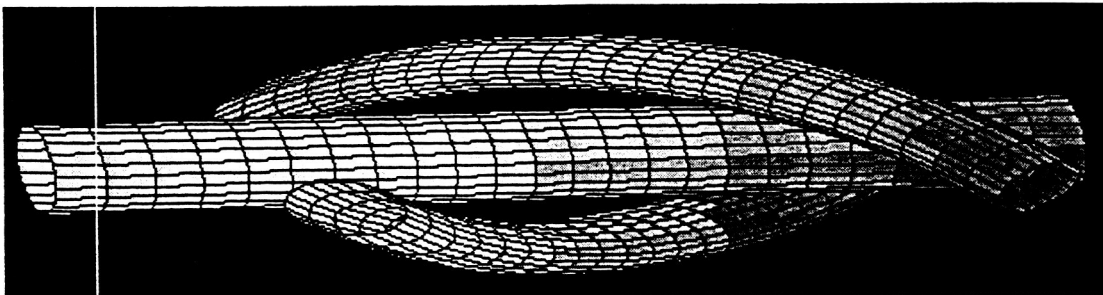Figure 5: Geometry of Triaxial Braid Model. *LSS*, Oblique View.

Figure 6: Geometry of Triaxial Braid Model. *LLS*, Front View.
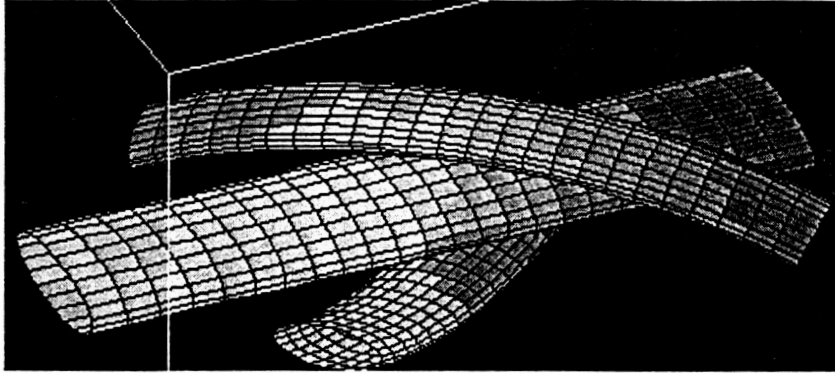
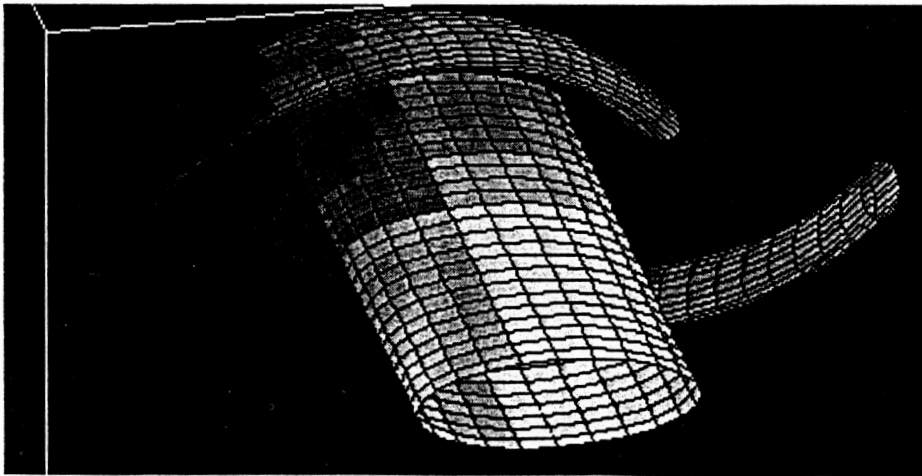Figure 7: Geometry of Triaxial Braid Model. *LLS*, Oblique View.

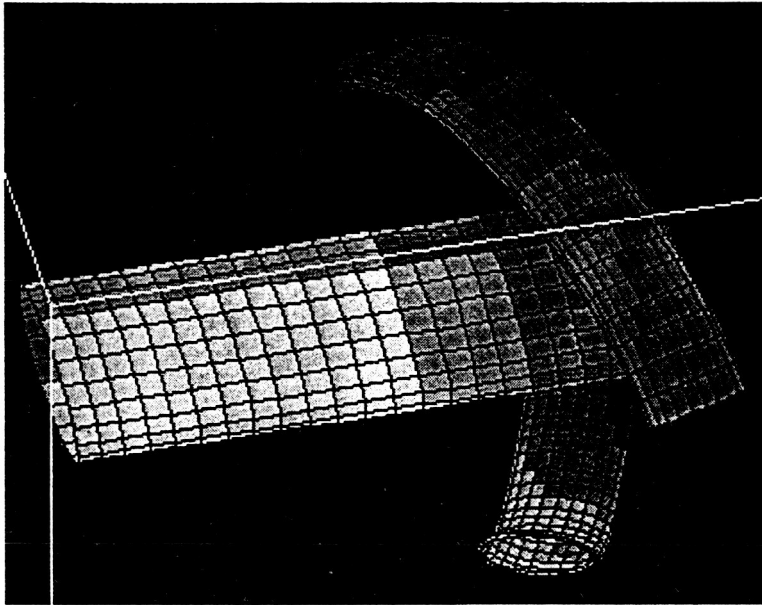Figure 8: Geometry of Triaxial Braid Model. *SLL*, Front View.

Figure 9: Geometry of Triaxial Braid Model. SLL, Oblique View.

As can be seen from the figures, neither mutual intersection nor gap between the yarns is seen for any of the four braids. Still the analysis of the numerical data shows the presence of a little gap (the biggest one is of about 1/5 of the minor radius length for SLL). The size of the gap depends upon the selection of penalty function imposed on the system in order to prevent mutual intersections of yarns and the number of iteration steps used for convergence analysis. The size of this gap can be controlled by changing the penalty function. For the current results, the penalty function had a "near-field" component acting as a repulsive force when the yarns are close enough. It was introduced in order to reach fast convergence to the equilibrium state. Thus the price for reduction of the slot between the yarns which are supposed to touch one another will always be a slower convergence.

EXPERIMENTAL METHODS FOR DETERMINING GEOMETRIC FEATURES

Experimental methods for evaluating and quantifying geometric features generally fall into two classifications: destructive and non-destructive. Work has been carried out in both of these activities, and a brief description of the techniques and typical results follows.

Material Serial Sectioning

The specimen preparation is carried out by mounting a small sample (1.0 x 1.0 x sample thickness) in a matrix cylinder (2.0 cm in diameter and 2.0 cm in height). Successive manual polishing operations are carried out to prepare the specimen for microscopical observation. The polishing operation is done with increasingly fine sandpaper, finishing with 1μm Al_2O_3 particles.

In order to get useful pictures for the three-dimensional image reconstruction, two main issues should be considered:

i. decreasing the distance between successive physical sections

ii. maintaining the levelness of each sample to ensure taking parallel pictures.

Coding pictures are carried out in two steps: first, Polaroid pictures directly from the microscope then digitizing the acquired pictures on computers using a flat bed scanner. Computer encoding for gray scale images is normally carried out by dividing the screen into small divisions

called pixels. Each pixel can be coded using the available gray scale range between black and white colors. This range can go up to 256 shades of gray. The values of gray can be used to distinguish yarn from surrounding resin.

Numerical Results

Figure 10 shows a stero pair rendering of serial cross-sectioning results from a triaxially braided fabric. For the purposes of clarity, only three yarns have been selected from the entire fabric. The fabric underconsideration was "A-1" from the NASA Langley research project, a triaxially braided carbon/epoxy composite with a nominal braid angle of 65°.
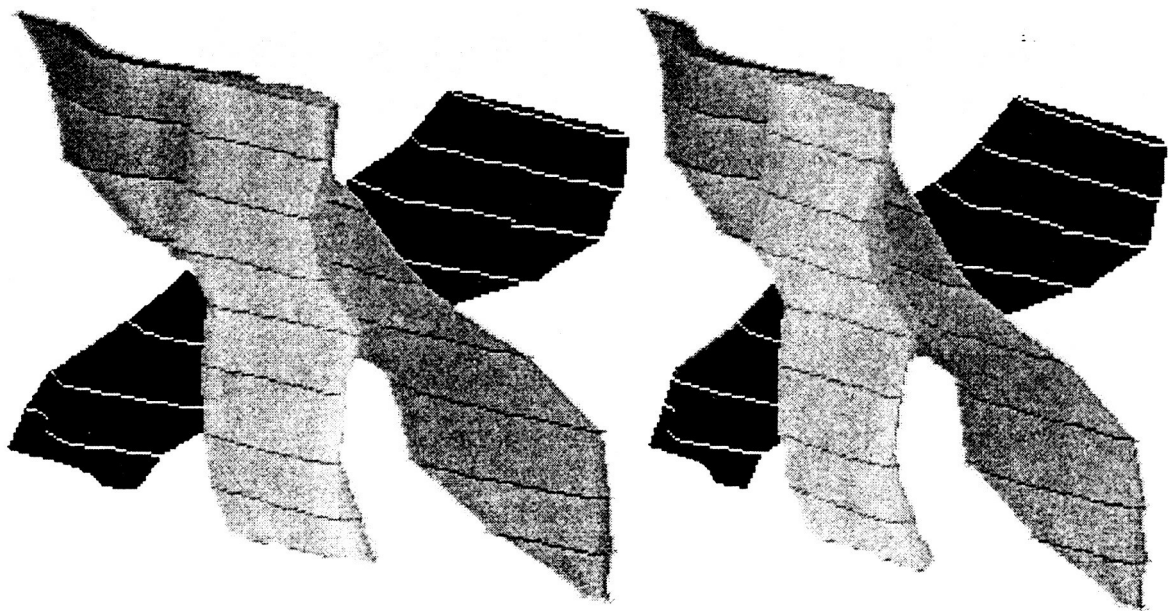
Figure 10: Stero Pair Rendering of Serial Section Imaging of Braid $A - 1$ showing Three Yarns in the Fabric

Modelling of the geometrical reinforcement requires some experimental activities to validate the work. The use of established conventional x-radiography is in principle attractive for this purpose but requires enhancement of the yarns since graphite and epoxy are both transparent to standard operating voltages. Investigations into two different methods show that enhancement can be accomplished and yarn detection is possible. One approach attempts to image the entire yarn body via doping with materials of high x-ray attenuation. The other utilizes radiographically opaque tracer fibers in the individual yarns to determine global yarn orientations. The use of doped prepreg fibers and copper magnet wire for tracers produced the best results for each respective method.

The established and low-cost non-destructive imaging techniques of conventional radiography and computed tomography (CT) are attractive for this application, save for some fundamental problems. Graphite and the constituent materials of epoxy have low atomic numbers (¡22) and are basically transparent to the operating voltages of conventional radiography (typically over 50 kV). X-rays exhibit a linear increase in mass attenuation with respect to rising atomic number. This results in denser materials providing greater contrast in a radiograph. In addition, the yarn and matrix have similar x-ray attenuation coefficients (3.22 *barns* for carbon versus 3.50 *barns* for typical epoxies at 80 kV energy) resulting in no visible contrast between the two in a radiograph. The first problem has been overcome via the use of soft, high flux x-rays operating at 10-20 kV which will image graphite-epoxy but require special equipment and dealing with problems such as air becoming a predominant absorber. Even with this technique, the yarns are still difficult to distinguish which prevents the tracing of the yarns with CT.

In order to utilize conventional x-radiography operating levels, it is necessary to enhance the yarns in some fashion to increase their contrast, both to the radiation and to the epoxy matrix. Since the primary concern of this study was to image the yarns, the matrix was not modified and left transparent to the x-rays.

Two approaches were examined to enable the determination of yarn orientation. The first involved the doping of individual yarns with substances possessing high attenuation coefficients. This was aimed at imaging the entire yarn in width and length in a radiograph and in cross-section with tomography. The second approach examined the introduction of radiographically opaque tracer fibers into the graphite yarns. Although the actual yarn would not be imaged, the idea was to determine yarn direction on a global scale.

Samples for this study consisted of six 12K graphite yarns unidirectionally woven with a continuous T40 Kevlar fill. Epon 8132 resin with V-40 hardener was used for the matrix at a 1:2.5 mix ratio. Individual yarns were treated before weaving.

Modifications to individual yarns for each sample were as follows:

Sample 1	10% concentration of Gadolinium Oxide powder in RIMline GMR-5000 Polyurethane resin applied to fibers, prepreg formed and un-doped Epon resin used to consolidate part.
Sample 2	Yarns sprayed with 3-M 77 adhesive, coated with Gadolinium Oxide powder and overcoated with 77 adhesive.
Sample 3	Yarns sprayed with 3-M 77 adhesive, coated with Boric Acid powder and overcoated with 77 adhesive.
Sample 4	10% concentration of Gadolinium Oxide powder in Acetate solution; yarns immersed for 10 seconds and Acetate dried off; 77 adhesive overcoat applied.
Sample 5	10% concentration of Gadolinium Oxide powder in Acetate solution; yarns immersed for 10 seconds and Acetate dried off; no overcoat applied.
Sample 6	40 AWG copper magnet wire (113 μm diameter) laid with three yarns before weaving.
Sample 7	37 AWG copper magnet wire (78 μm diameter) laid with three yarns before weaving.
Sample 8	100 μm boron fibers laid with three yarns before weaving.
Sample 9	Control

The choices for enhancement substances were made in regard to neutron radiography as well as x-ray radiography, the gadolinium and boron materials being high neutron absorbers. Results from the neutron radiography work will be reported next quarter.

A Picker model F-12 x-ray tube rated at 50-90 kV and 0-15 mA was used for exposures with Kodak SR-5 industrial radiographic film. No back screen was employed. Distance between tube opening and the image plane was 34 inches. Timed step wedges were made at different combinations of voltage and flux to determine a background optical density of 2.5 for the film. The final settings were 80 kV and 4.5 mA for 45 second exposure.

For the first approach of enhancing the entire yarn, Sample 1 produced the best radiograph. The individual yarns are clearly distinguished with good edge and spatial resolution. By prepreging individual yarns, the enhancing material is somewhat constrained within the dimensional boundaries of the yarn and has less of a chance to diffuse into the surrounding matrix, thus blurring the image. However, this method makes yarn-fabric processing difficult since partly cured resin stiffens the yarn and allows less freedom for detailed geometries.

Some demarcation between the yarns and the matrix could be seen in Sample 2 though it is interesting to note that the "thin shell" phenomena exists with the coatings. Whereas the yarns appear lighter than the matrix in Sample 1, in Sample 2 the spacing between the yarns is the lighter area. This is effectively the contact area between the yarns where the thickness of gadolinium oxide is greatest, thus imaging the yarn edges. One thought to this would be to dope the matrix with an enhancer and look for the yarns. Unfortunately, the epoxy already has a slightly higher x-ray attenuation than raw carbon and any further increase would fully mask the presence of the yarns.

Samples 4 and 5 also showed visible contrast of the yarns although soaking the yarns in the acetate solution dissolved the yarn sizing. This allowed the yarn fibers to blossom making the parts difficult to process and resulting in irregular yarn dimensions in the radiographs. The adhesive applied to Sample 4 had no effect in constraining the fibers. The distribution of gadolinium oxide in the yarns is random, probably due to the position of the yarns during draining of the solution. With further development of this technique including the application of sizing after the solution, improved results may be possible.

The boric acid sample and the control did not produce radiographs with sufficient contrast for reproduction. The boron samples (both powder and fibers) hold more potential for contrast with neutrons as the transmission medium.

Tracer Fibers

Both the 40 and 37 AWG magnet wires in Samples 6 and 7 were easily distinguished. Though the yarns were not discerned, their paths and orientations were readily evident. Attractive features of the magnet wire included its ease of processing, size, ductility and low cost. The idea for using

tracer fibers in composites has been investigated for some time though typically plies rather than individual yarns are the topic of interest and the tracer fibers usually have mechanical properties similar to the graphite yarns. In this study, tracers were solely used for imaging purposes and not for mechanical testing.

The boron fibers in Sample 8 were discernible though not nearly to the extent of the copper wires. The contrast was probably due to the tungsten core of the boron fibers. Again, the boron fibers should contrast stronger with neutron radiography though their expense and difficulty in processing may make their application impractical.

MECHANICAL PROPERTY PREDICTIONS

One of the objectives of determining the geometric properties of textile reinforcements is to provide a means to understand the mechanical response of the composite formed from the fabric. Since the mechanical properties of a continuous fiber reinforced composite are clearly highly dependent upon .geometric properties, it is necessary to understand the structure of the reinforcement in order to carry out any property predictions.

Two basic approaches to this problem were employed. In one case the geometric data were used as input to a meshing algorithm creating a finite element model of the yarns and surrounding matrix. In the other the geometric data was reduced to simpler orientation parameters and a smearing method was employed.

Application to FEA Methods

Working with Hayden Griffen and Edward Glaesgen from VPI&SU, conversion of the geometric data for finite element modelling was carried out. Once the yarn cross section and spline data are obtained from the TGM, they are directly converted to a format suitable for use in SDRC I-DEAS 6.1[2]. First, the cross section of the yarn is input as a series of discrete points on the yarn surface. These points are fit to a B-spline representing the yarn perimeter [9]. Second, the yarn center line points are input and fit to a B-spline in a similar manner. The I-DEAS skin group for the yarns is developed by first creating a profile from the B-spline fit yarn cross section. This profile is dragged along the cross sectional spline to develop the yarn skin group.

---

[2] Available from Structural Dynamics Research Corporation, Milford, OH

The solid modeling feature in I-DEAS is used to translate the yarn skin group to a yarn solid object. Creation of additional yarns proceeds in one of two ways. If an additional yarn is merely a translated or rotated version of the original, the appropriate I-DEAS commands are executed to perform the translation/rotation operation. If the yarn is unique (not a translated or rotated version of a previous yarn), the original yarn creation process is repeated beginning with the surface and/or spline points.

The outer boundaries of the representative volume element (RVE) are represented as a hexahedral shaped solid object oriented with its centroid at the centroid of the RVE. The boolean capabilities within I-DEAS are used to subtract the yarns from the outer block. The object that remains corresponds to the surrounding matrix contained within the RVE.

Once the RVE solid containing the details of the interior boundaries of the textile has been developed, the mesh area and mesh volumes are created. The original volume is considered matrix material, while the yarn volumes become yarn finite element volumes.

Stiffness Averaging

Another approach to simple mechanical property predictions is through the use of homogenization techniques for predicting constituitive relations for the material under investigation.

The Fabric Geometry Model (FGM) is a technique for predicting the stiffness of composite materials with spatially oriented reinforcements. This technique, developed by the authors and their colleagues [10] [11] [12], calculates elastic properties from constituent material properties using micromechanics and geometrical properties of textile reinforcement. The objective of this paper is to present a Self-Consistent FGM model which can be easily adopted by researchers in this area. The particulars of the calculations are demonstrated and sample pseudo-code is given for the development of software. The objective of the model is to allow designers to identify composite properties from constituent material properties and the textile processing route. Although lacking the detail of more rigorous finite element techniques, such as those developed by [13] and [14], the FGM provides a quick method for constructing good predictions of elastic behavior. With additions to the approach, strain dependent tensile behavior can be modeled, such as that associated with metal matrix composites (plastic deformation of matrix [15]) and ceramic matrix composites (micro-cracking of matrix [16]).

The basic idea behind the FGM is to treat the fibers and matrix as a set of composite rods having various spatial orientations. The local stiffness tensor for each of these rods is calculated and rotated in space to fit the global composite axes. The global stiffness tensors of all the composite rods are then superimposed with respect to their relative volume fraction to form the composite stiffness tensor. This technique is called a stiffness averaging method [17].

Formulation Of Transformation Tensor

The transformation of the local stiffness matrix to the global stiffness matrix is as follows [18] :

$$C_{global} = T_\sigma^{-1} \; C_{local} \; T_\epsilon \tag{4}$$

where C_{global} and C_{local} are the global and local stiffness matrices respectively and T_σ and T_ϵ are the stress and strain transformation matrices successively.

We can write [19]:

$$T_\epsilon = \begin{pmatrix} l_1^2 & l_2^2 & l_3^2 & l_2 l_3 & l_1 l_3 & l_1 l_2 \\ m_1^2 & m_2^2 & m_3^2 & m_2 m_3 & m_1 m_3 & m_1 m_2 \\ n_1^2 & n_2^2 & n_3^2 & n_2 n_3 & n_1 n_3 & n_1 n_2 \\ 2m_1 n_1 & 2m_2 n_2 & 2m_3 n_3 & m_2 n_3 + m_3 n_2 & m_1 n_3 + m_3 n_1 & m_1 n_2 + m_2 n_1 \\ 2l_1 n_1 & 2l_2 n_2 & 2l_3 n_3 & l_2 n_3 + l_3 n_2 & l_1 n_3 + l_3 n_1 & l_1 n_2 + l_2 n_1 \\ 2l_1 m_1 & 2l_2 m_2 & 2l_3 m_3 & l_2 m_3 + l_3 m_2 & l_1 m_3 + l_3 m_1 & l_1 m_2 + l_2 m_1 \end{pmatrix} \tag{5}$$

Due to orthogonality, T_σ and T_ϵ have the following relation [19]

$$T_\sigma^{-1} = T_\epsilon^T \tag{6}$$

and we need to determine T_ϵ only.

Although the transformation tensors are well defined, the actual technique of determining the values of the transformation matrices for stresses (T_σ) and the strains (T_ϵ) are not consistent in the literature. Furthermore, some formulations are not defined over all possible orientations. The authors recommend the following procedure.

The formation of the transformation matrices depends exclusively on the direction cosines l_i, m_i, and n_i. These direction cosines may be viewed as the components of the unit basis vectors associated with the principal axes of the fibrous reinforcement:

- $\vec{r_1}$ = unit vector associated with the fiber axis = (l_1, l_2, l_3)

- $\vec{r_2}$ = unit vector associated with the #2 direction of the fiber = (m_1, m_2, m_3), and

- $\vec{r_3}$ = unit vector associated with the #3 direction of the fiber = (n_1, n_2, n_3).

In most instances, $\vec{r_1}$ is known. This may be determined by constructing a rectangular parallelepiped which contains the fiber, having dimensions a, b, and c. In this case, $\vec{r_1}$ can be determined as:

$$\vec{r_1} = \frac{a}{\sqrt{a^2 + b^2 + c^2}} \; \vec{\imath} \; + \; \frac{b}{\sqrt{a^2 + b^2 + c^2}} \; \vec{\jmath} \; + \; \frac{c}{\sqrt{a^2 + b^2 + c^2}} \; \vec{k} \qquad (7)$$

Through the use of geometric relationships, it is possible to determine the other two vectors. Since $\vec{r_1}$, $\vec{r_2}$, and $\vec{r_3}$ are mutually orthogonal,

$$
\begin{aligned}
\vec{r_1} \bullet \vec{r_2} &= 0 \\
\vec{r_2} \bullet \vec{r_3} &= 0 \\
\vec{r_1} \bullet \vec{r_3} &= 0
\end{aligned}
\qquad (8)
$$

where $\vec{x} \bullet \vec{y}$ = inner product (dot product) of vectors $\vec{x}$ and $\vec{y}$. As they are all direction cosine vectors, they have modulus of unity:

$$
\begin{aligned}
\|\vec{r_1}\| &= 1 \\
\|\vec{r_2}\| &= 1 \\
\|\vec{r_3}\| &= 1
\end{aligned}
\qquad (9)
$$

Since the unidirectional fiber is transversely isotropic, there is one degree of freedom in the determination of $\vec{r_2}$ and $\vec{r_3}$. This degree of freedom was employed by the authors as:

.

$$m_1 = \sqrt{1 - l_1^2} \qquad (10)$$

Since l_1 is the direction cosine of the fiber with the x-axis ($cos(1, x)$), the definition of m_1 corresponds with $m_1 = sin(1, x)$. This places the 2-axis of the fiber in the plane made with the fiber and the x-axis of the composite. The remaining 5 terms can be solved from 8 and 9. Of course, it is important to use the relationships in 8 for the determination of the last term in each vector and to account for the radical term introduced by 10. A sample pseudo-code solution algorithm for determining the numerical value of these three vectors is given in Figure 11.

Then, for each system of reinforcing fibers, the global stiffness C_{global_i} is calculated and the total composite stiffness is determined as:

$$C_{comp} = \sum_{i=1}^{n} k_i C_{global_i} \qquad (11)$$

where C_{comp} is the composite final stiffness matrix and k_i is the relative volume fraction of the ith reinforcing system.

This technique is called a "stiffness averaging" method [17]. Alternatively, one may use the "compliance averaging" method, in which case the composite stiffness is determined by :

$$C_{comp}^{-1} = \sum_{i=1}^{n} k_i C_{global_i}^{-1} \qquad (12)$$

Conclusions

The quantification of the geometric structure of a fabric can be accomplished for an idealized system. The incorporation of defects, deformations, and distortions raises the complexity of the problem tremendously.

The availability of the geometric data provides a mechanism for developing analytical methodologies to predict mechanical properties of the reinforced structure. Even in the event of idealization of the reinforcing geometry, such an approach has a significant pedagogical value to research.

References

[1] Frank K. Ko and Christopher M. Pastore. Cim of braided preforms for composites. In C. A. Brebbia, W. P. deWilde, and W. R. Blain, editors, *Computer Aided Design in Composite Materials Technology*. Springer-Verlag, 1990.

[2] Christopher M. Pastore, Yasser A. Gowayed, and YunJia Cai. *Applications of Computer Aided Geometric Modelling for Textile Structural Composites*, pages 45–53. Computational Mechanics Publications, Southampton, UK, 1990.

[3] I.S. Raju, R. L. Foye, and V. S. Avva. A review of analytical methods for fabric and textile composites. In *Proceedings of Indo-US Workshop on Composite Materials for Aerospace Applications*, July 1990.

[4] H. B. Dexter, E. T. Camponeschi, and L. Peebles. 3-d composite materials. NASA Conference Pubvlication 24020, Hampton, VA, November 1985.

[5] K. Woo and J. D. Whitcomb. Global/local finite element analysis for textile composites. In *34th AIAA/ASME/ASCE/AHS/ACS Structures, Structural Dynamics and Materials Conference*, pages 1721-1731, La Jolla, CA, 1993. AIAA/ASME/ASCE/AHS/ACS.

[6] F. T. Pierce. The geometry of cloth structures. *Journal of the Textile Institute*, 28, 1937.

[7] P. Bézier. *Essay de définition numérique des courbes et des surfaces expérimentales*. PhD thesis, University of Paris VI, 1977.

[8] P. E. Bezier. A computer aided system for car body design. In K. B. Evans and E. M. Kidd, editors, *Proceedings of Graphics Interface '82*, pages 131-152, 1982.

[9] A. W. Tiller. Rational B-splines for curve and surface representation. *IEEE Computer Graphics and Applications*, pages 61-69, September 1983.

[10] Dennis W. Whyte. *On the Structure and Properties of 3-D Braided Composites*. PhD thesis, Drexel University, Philadelphia, PA, June 1986.

[11] Christopher M. Pastore. *A Processing Science Model of Three Dimensional Braiding*. PhD thesis, Drexel University, Philadelphia, PA, March 1988.

[12] Frank K. Ko and Christopher M. Pastore. Design of complex shaped structures. In *Textiles: Product Design and Marketing*, pages 123-135. The Textile Institute, The Textile Institute, May 1987.

[13] R. L. Foye. Finite element analysis of unit cells. In J. Buckley, editor, *Fiber Tex '90*, pages 45-53, Hampton, VA, May 1992. NASA Langley Research Center, NASA Langley Research Center.

[14] J. D. Whitcomb. Three dimensional stress analysis of plain weave composites. In *3rd Symposium on Composite Materials: Fatigue and Fracture*, Philadelphia, PA, Oct. 1989. American Society for Testing and Materials, ASTM.

C6-5.

[15] Frank K. Ko, Christopher M. Pastore, Charles Lei, and Dennis W. Whyte. A fabric geometry model for 3-D braid reinforced FP/Al-Li composites. In *1987 International SAMPE Metals Conference: Competitive Advances in Metals/Metal Processing*, Cherry Hill, NJ, Aug. 1987. American Society for Testing and Materials, ASTM.

[16] Christopher M. Pastore, Eileen Armstrong, and Frank K. Ko. A fabric geometry model for brittle matrix composites. In *Ceramic Matrix Composites*, Indianapolis, IN, April 1989. American Ceramic Society, ACerS.

[17] A. F. Kregers and G. A. Teters. Use of averaging methods to determine the viscoplastic properties of spatially reinforced composites. *Polymer Mechanics*, 15(4):617–624, July-August 1979.

[18] George E. Dieter. *Mechanical Metallurgy*. McGraw-Hill Book Co., New York, third edition, 1986.

[19] A. E. H. Love. *A Treatise on the Mathematical Theory of Elasticity*. Dover Publications, New York, 4 edition, 1944.